Carbon 126 (2018) 464–471

Contents lists available at ScienceDirect

Carbon

journal homepage: www.elsevier.com/locate/carbon

Flexible thermal rectifier based on macroscopic PDMS@graphite composite film with asymmetric cone-shape interfaces

Bensong Chen [a, b], Matthieu Pawlik [c], Roland Yingjie Tay [b], Minmin Zhu [d], Manuela Loeblein [d], Siu Hon Tsang [b], Edwin Hang Tong Teo [d, e, *]

[a] Key Laboratory of Materials Physics, CAS Center for Excellence in Nanoscience, Anhui Key Laboratory of Nanomaterials and Nanotechnology, Institute of Solid State Physics, Chinese Academy of Sciences, Hefei 230031, PR China
[b] Temasek Laboratories, Nanyang Technological University, 50 Nanyang Avenue, 639798, Singapore
[c] CNRS-International-NTU-Thales Research Alliance, Nanyang Technological University, 50 Nanyang Avenue, 639798, Singapore
[d] School of Electrical and Electronic Engineering, Nanyang Technological University, 50 Nanyang Avenue, 639798, Singapore
[e] School of Materials Science and Engineering, Nanyang Technological University, 50 Nanyang Avenue, 639798, Singapore

ARTICLE INFO

Article history:
Received 22 March 2017
Received in revised form
1 July 2017
Accepted 14 October 2017
Available online 15 October 2017

ABSTRACT

Thermal rectifier is a device with the higher heat transport capacity in one direction than the backward one, being similar to the electrical diode working for the control of the electrical current. In this work, we report a new thermal rectifier based on the flexible macroscopic polydimethylsiloxane (PDMS) film with asymmetric cone-shape holes embedded with micrometer sized graphite powder (denoted as PDMS@graphite). The PDMS@graphite shows thermal rectification behavior with an extracted thermal rectification coefficient of 1.1326 ± 0.009 under 129.8 K temperature bias, and this value can be further modulated by changing the asymmetric ratio of the cone-shape interface in the PDMS@graphite film. Two underlying mechanisms are invited to explain the thermal rectification effect in the PDMS@graphite system. The one is the opposite temperature dependence of thermal conductivity for PDMS and graphite powder. The other one is the different temperature dependent thermal conductivity of the asymmetric cone-shape graphite in PDMS@graphite film in the forward and backward heating direction when applying the same temperature bias, which can be demonstrated in the COMOSL theoretical simulated temperature distributions for the PDMS@graphite. The as-fabricated flexible macroscopic PDMS@graphite composite film thermal rectifier may provide the potential applications in thermal control and management.

1. Introduction

Thermal rectifier refers to a device with the distinct heat flow capacity along the different (*i.e.* forward and backward) directions, being analogous to the modulation of electrical current in a p-n junction of an electrical diode. Because of its ability to effectively modulate heat transport, thermal rectifiers are often used in many thermal-based devices such as thermal logic gate [1], thermal transistor [2] and thermal memory [3]. Regardless of the type of energy carrier (electron, phonon, and photon) of heat conduction in material, asymmetricity and nonlinearity of energy transport is essential to realize the thermal rectification effect in material system. To date, great efforts have been made in the theoretical or experimental aspects to realize the thermal rectification effect in both nanostructured and bulky material systems. As the dimensions of the nanomaterials approach to the characteristic wavelength of phonon in lattice vibration, the phonon will be scattered at the interfaces or boundaries of nanostructures, leading to the changes of phonon mean free path and the thermal conductivity of nanomaterials. Thus, designing nanomaterials with particular asymmetric structures may offer the opportunities to obtain the thermal rectification effect. For example, thermal rectification phenomena have been theoretically predicted in various asymmetric nanostructures, which include asymmetric nanowires [4], telescopic shape silicon nanowires [5], carbon nanocone [6], deformed carbon nanohorns [7], asymmetric graphene ribbons [8], three-terminal graphene nanojunctions [9] and graphene Y-

* Corresponding author. School of Materials Science and Engineering, Nanyang Technological University, 50 Nanyang Avenue, 639798, Singapore
E-mail address: HTTEO@ntu.edu.sg (E.H.T. Teo).

https://doi.org/10.1016/j.carbon.2017.10.046
0008-6223/

junction [10]. In addition, the thermal rectification effects have also been experimentally realized in asymmetric nanostructures such as a tapered shape vanadium dioxide nanowire [11] and a single mass-gradient carbon nanotube with the deposition of $C_6H_{16}Pt$ [12]. Although many progresses have been experimentally realized the thermal rectification effect in nanosystems, it is still difficult to fabricate such asymmetric nanostructures and further measure their thermal properties on the micro/nano devices.

As the bulky materials are more easily to be processed and further test their thermal property, it can be specially designed to acquire the thermal rectification effect through using different approaches: (1) To search structural phase transition materials accompanying with a rapid change of thermal conductivity at the phase transition temperature. Pallecchi et al. [13] designed a thermal diode basing on a phase changing material and realized a proof-of-concept device consisting of a series of poly(N-isopropylacrylamide) (PNIPAM, the phase changing material) and polydimethylsiloxane (PDMS). Chen et al. [14] reported the achievement of controllable thermal rectification effect in binary phase change composites of eicosane/PEG 4000 stuffed reduced graphene oxide (rGO) aerogel. (2) To form a composite consisting of two kinds of materials possessing thermal conductivities with different temperature dependence. Kobayashi et al. [15] reported the oxide thermal rectifier made of two cobalt oxides ($LaCoO_3$ and $La_{0.7}Sr_{0.3}CoO_3$) with the opposite trends in their temperature dependence of the thermal conductivity. Accordingly, obvious thermal rectification phenomenon has also been observed in the macroscopic asymmetric pyramid shape two-segment $LaCoO_3$/$La_{0.7}Sr_{0.3}CoO_3$ oxide material system [16]. Furthermore, Li et al. [17] designed a kind of macroscopic thermal diode based on temperature-dependent transformation thermotics. Although different types of bulky thermal rectifier have been successfully fabricated, there are still some shortcomings hinder their practical applications. For example, most of the reported macroscopic thermal rectifiers are difficult to be scaled up and also are rigid rather than flexible, which may be important in some specific application occasions. Up to date, different kinds of bulky flexible thermal rectifiers have been experimentally realized, including asymmetric geometry parallel aligned and interconnected graphene composites film [18] and triangle-shape paper-like rGO film [19]. However, these reported macroscopic thermal rectifiers can only realize the thermal rectification effect in the in-plane (*x*-*y*) direction. Therefore, it is necessary to develop an effective method to fabricate flexible macroscopic thermal rectifier with the conveniences to scaling up and the capacity of modulating the heat flow perpendicular to the in-plane (*i.e.* vertical z) direction, which may bring the new applications in thermal management under particular circumstances.

In this work, we mainly focus on the possibilities to realize the flexible bulky thermal rectifier with the capacity to effective control the heat flow in the vertical *z* direction. To achieve this goal, we want to utilize the above mentioned approach (2) to obtain the thermal rectification effect. On one hand, we try to assemble a composite thermal rectifier consisted of two kinds of materials A and B having the thermal conductivity with opposite trend of temperature dependence. On the other hand, we make the two constituent materials of the composite have asymmetric shape and also possess asymmetric interface between them. By taking use of the asymmetric shape interface between the two materials A and B, different temperature distributions can be respectively formed in the material A or B under the forward and backward heating direction when applying the same temperature bias. Since the averaged thermal conductivity of materials A and B is temperature dependent, the corresponding different temperature distributions in the asymmetric shape materials A and B can further induce the distinct averaged thermal conductivity for materials A or B in the forward and backward heat flux directions and finally thermal rectification effect in this two-component A/B material system. The design intent for the thermal rectifier is shown in Scheme 1. Considering the flexibility and large scale processing conveniences for the thermal rectifier, we choose polymer as the base material. PDMS is a kind of useful silicon based polymer widely used in the electronic [20] and biological [21] fields. PDMS possesses the advantages of good chemical inertness, almost non-toxicity and feasibility to be processed in the desired shape and structure. Thus, PDMS film is an ideal candidate to fabricate flexible film with desired asymmetric structure. Herein, we firstly prepare a macroscopic solid-state PDMS film with the asymmetric cone shape holes through using the metal mold with the pre-designed structure. Then, micrometer sized graphite powder is filled and packed in the cone shape holes of the as-prepared PDMS film (denoted as PDMS@graphite) by copper foil tape to obtain thermal rectification effect in terms of the graphite powder and PDMS film showing the opposite temperature dependence trend for the thermal conductivity (discussed in the below details). Therefore, the above mentioned approach (2) is utilized in the PDMS@graphite composite film. By applying the same temperature bias on the planar top and bottom surface of PDMS@graphite film, larger heat flux transferring across the sample can be detected in the negative heating direction than that of positive heating direction, which implies the thermal rectification effect in the PDMS@graphite film. The experimental thermal rectification coefficient of the resultant PDMS@graphite composite film is 1.1326 ± 0.009 under 129.8 K temperature bias and modulated by tuning the asymmetricity ratio (cone angle) of the cone-shape graphite powder in the sample. Benefiting from the asymmetric cone-shape interfaces between the PDMS and graphite in the PDMS@graphite, different temperature gradient distribution induced thermal conductivity differences are generated in the PDMS@graphite under the same temperature bias in the different heating directions, which can be well demonstrated in the theoretical simulations of temperature distribution in the PDMS@graphite. The as-prepared flexible asymmetric structured macroscopic PDMS@graphite composite film may provide the reference to design thermal rectifier and show the possible applications in thermal control or management.

2. Experimental

2.1. Materials

The precursors for preparation of PDMS solution are silicone elastomer base and curing agent (Sylgard 184). Graphite powder (Sigma-Aldrich Co. Ltd., diameter smaller than 20 μm), copper foil tapes (Latech Scientific Supply Pte. Ltd., thickness 0.055 mm) and all chemicals were used as received without further purification.

Scheme 1. The schematic design for the thermal rectifier composed of two different materials with asymmetric shape and interfaces.

2.2. Preparation of PDMS film with cone-shape holes

Initially, we designed a typical aluminum (Al) mold with totally sixteen (4 × 4) same sized cones (cone angle $\Theta = 60^{\circ}$) which are evenly distributed on one planar surface and surrounded by the square frame. Then, a fully homogeneous mixture of silicone elastomer base and curing agent (Sylgard 184, volume ratio 10: 1 at room temperature) was cast into the Al mold and stood for 1 h to fully eliminate the air bubbles in the PDMS solution. Afterward, the Al mold containing with the PDMS solution was heated up to 80 °C and kept for 5 h in an oven. After the treatment, the PDMS solution would be polymerized and solidified in the Al mold so as to form solid-state PDMS film and then can be peeled off from the Al mold to get the solid-state PDMS film with the cone-shape holes.

3. Results and discussion

3.1. Preparation of the PDMS@graphite composite film

The fabrication procedure for the PDMS@graphite composite film is schematically shown in Fig. 1. Briefly, a solid-state PDMS film with cone-shape holes (total number is sixteen) was initially prepared by using an Al mold with the pre-designed structure. Subsequently, micrometer sized (diameter smaller than 20 μm) graphite powder was filled and packed in the cone-shape holes of as-obtained PDMS film by adhering copper foil tapes (0.055 mm thickness) on the planar surfaces of PDMS film. The optical photography of the as-fabricated Al mold and solid-state PDMS film with cone-shape holes is displayed in the left and right part of Fig. 2a, respectively. It should be pointed out that the liquid level of the PDMS solution casted into the Al mold should not exceed the tips of cones (schematically shown in Fig. 1), which can ensure the cone-shape holes of the as-prepared PDMS film are through-hole. Typically, we fabricate the PDMS@graphite with the cone angle 60°. Fig. 2b and c clearly show the three-dimensional (3D) schematic views of the detailed geometrical sizes and spatial distribution of the cone-shape graphite (cone angle $\Theta = 60^{\circ}$) dispersed in the PDMS@graphite sample.

3.2. Measurement of the thermal rectification effect of the PDMS@graphite

In order to measure the possible thermal rectification effect in the PDMS@graphite, we designed and made a customized testing setup. Fig. 3 displays the cross-sectional schematic view of the measurement part of the apparatus, which is basically symmetric structure from top to bottom. It is composed of two sets of supporting plates, two pieces of thermal insulators, two heater/cooler blocks and a testing PDMS@graphite composite sample located in the central part. To ensure the good thermal contact, these units are assembled and pressed tightly by the screws following the spatial sequence schematically shown in Fig. 3. The two sets of thermal insulators are respectively installed adjacent to the top and bottom supporting plate to prevent the heat leakage. The heater/cooler can be used as either heater (electrical heater, with the electrical resistance $r = 7.0\ \Omega$) or cooler according to the experimental needs. The cooler units are the copper pipes coil connected to the circulating cooling water (constant temperature 5 °C) at the flow rate 0.2 L min^{-1}. Thermocouples with 25 μm diameter are put on the top and bottom surface of the PDMS@graphite composite sample to monitor the corresponding sample surfaces temperature in the testing process. To minimize the convective heat leakage into the environment, the entire measurement apparatus is enclosed in a vacuum chamber which is evacuated down to 80 mTorr.

In the testing process, the top and bottom planar surface of the PDMS@graphite sample is respectively contacted to the heater and cooler so as to apply a temperature bias. Initially, the testing process started from the room temperature. Herein, we denote the positive heat flux direction when the larger diameter of cone-shape graphite in PDMS@graphite is at a higher temperature (facing to the heater), and the negative heat flux direction when the opposite smaller tip of cone-shape graphite in PDMS@graphite is at a higher temperature. In the following experimental steps, the heater in the system was program controlled and the corresponding input electrical currents (I) for the heater were also recorded in real time. With applying the electrical current for the heater, the top surface temperature of the sample increases accordingly. At the same time, the bottom surface temperature of the sample decreases as the bottom side is directly contacted to the cooler with the supply of the constant temperature circulating cooling water. After a certain period of time, the system can reach a non-equilibrium stationary state, *i.e.* both the top and bottom surface temperature of the sample arrive at a steady value. Fig. 4a shows the monitored top/bottom surface temperature of the PDMS@graphite sample as a function of time in the positive heating direction. The corresponding input electrical current for the heater is recorded and shown in Fig. 4b. For the macroscopic PDMS@graphite sample, the heat current density J through the sample follows the Fourier's law,

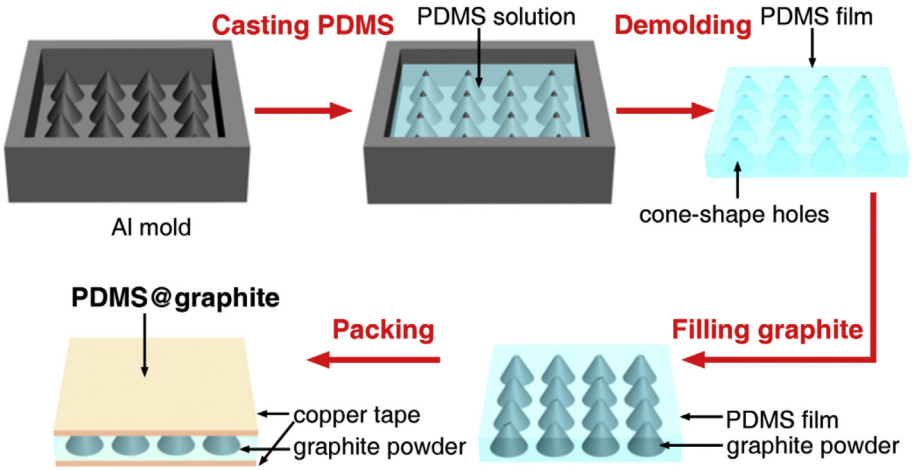

Fig. 1. The schematic fabrication procedure for the PDMS@graphite composite film. (A colour version of this figure can be viewed online.)

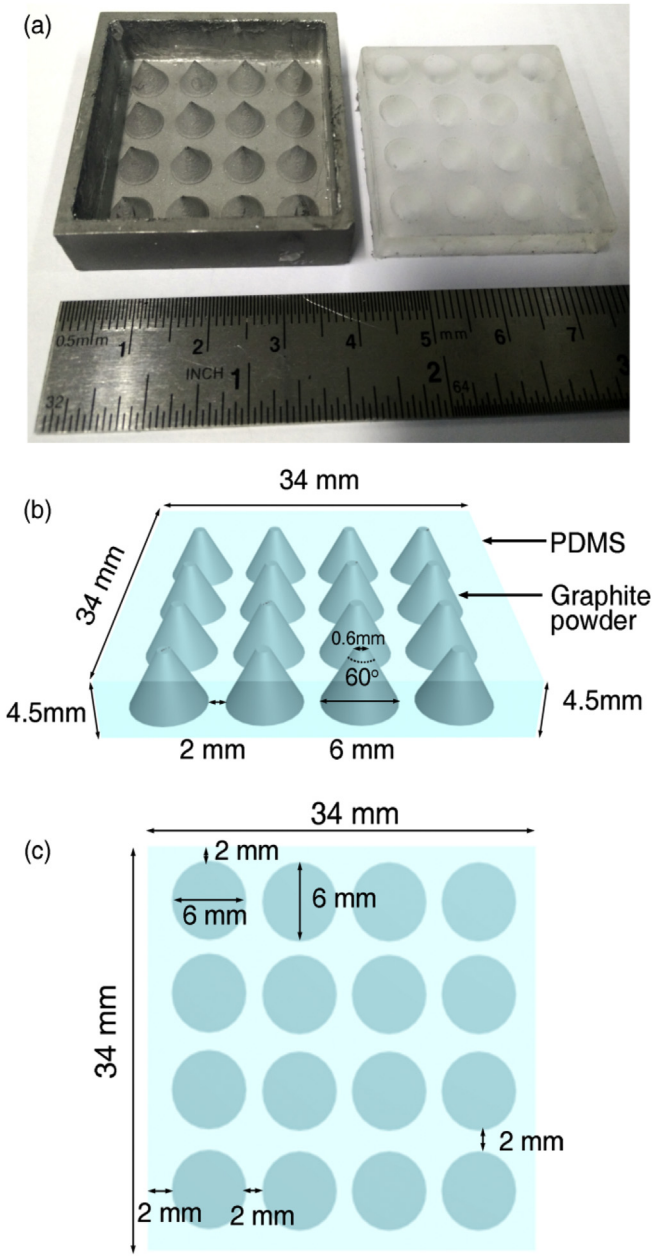

Fig. 2. (a) The optical photographs of the Al mold and the as-prepared solid-state PDMS film with cone-shape holes (angle $\Theta = 60^{\circ}$). The 3D schematic (b) side and (c) bottom view of the dimensions and distribution of graphite powder embedded in the PDMS film with cone-shape holes (cone angle $\Theta = 60^{\circ}$). (A colour version of this figure can be viewed online.)

which can be written as

$$J = -k[x, T(x)]\frac{dT(x)}{dx} \tag{1}$$

where, x is the position, $T(x)$ is the temperature at that position, k is the thermal conductivity of the PDMS@graphite sample as a function of position and temperature.

After finishing the thermal property testing for the sample under the positive heating direction, the PDMS@graphite sample was carefully turn over into the negative direction to make the smaller tips of the cone-shape graphite in the PDMS@graphite sample face to the heater. Additionally, all other experimental conditions were

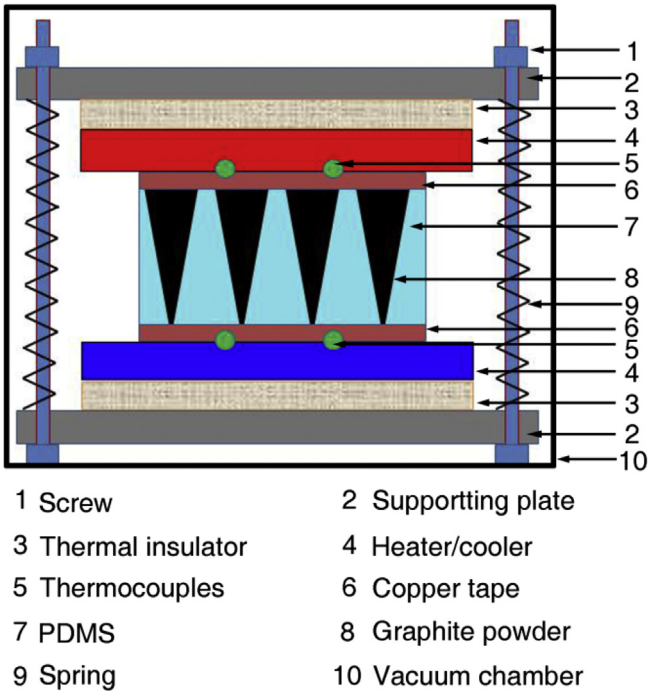

Fig. 3. The cross-sectional schematic of the measurement apparatus in the thermal rectification testing setup. (A colour version of this figure can be viewed online.)

kept unchanged except varying the input electrical current for the heater. To investigate if there existing thermal rectification effect in the PDMS@graphite composite system, the same stationary state temperature bias was also applied on the sample surfaces in the negative heating direction so as to compare the heat current density across the sample between the positive and negative direction.

In order to improve the thermal measurement accuracy, the thermocouples were put at the different positions on the planar top and bottom surfaces of PDMS@graphite, and meanwhile each thermal testing with different steady state forward/reverse temperature bias was conducted for ten times to check the thermal rectification effect in PDMS@graphite. In the measurement, the applied pressure will certainly influence the heat flux across the sample, which results from the pressure induced distinct shape change in our flexible PDMS@graphite composite sample. To precisely compare the heat current density across the PDMS@graphite samples between the forward and backward heating direction, the samples should be fixed in the testing setup with the same pressure when turning over the samples in the thermal measurement and applying the same reverse temperature gradient. In order to achieve this goal, the PDMS@graphite samples were assembled in the testing apparatus by using the screws with the same spring compression (schematically shown in Fig. 3), which can ensure the same pressure on the sample in the thermal measurements under the different heating directions. Thus, the thermal rectification coefficient R can be defined by the ratio of the negative heat current density ($|J_-|$) to the positive heat current density ($|J_+|$) across the sample:

$$R = \frac{|J_-|}{|J_+|} \tag{2}$$

If the value of R is equal to 1, it means no thermal rectification phenomenon in the PDMS@graphite composite system. The larger the value of R (if R>1.0), the higher the thermal rectification efficiency in the sample. In the negative heat flux direction, the heater

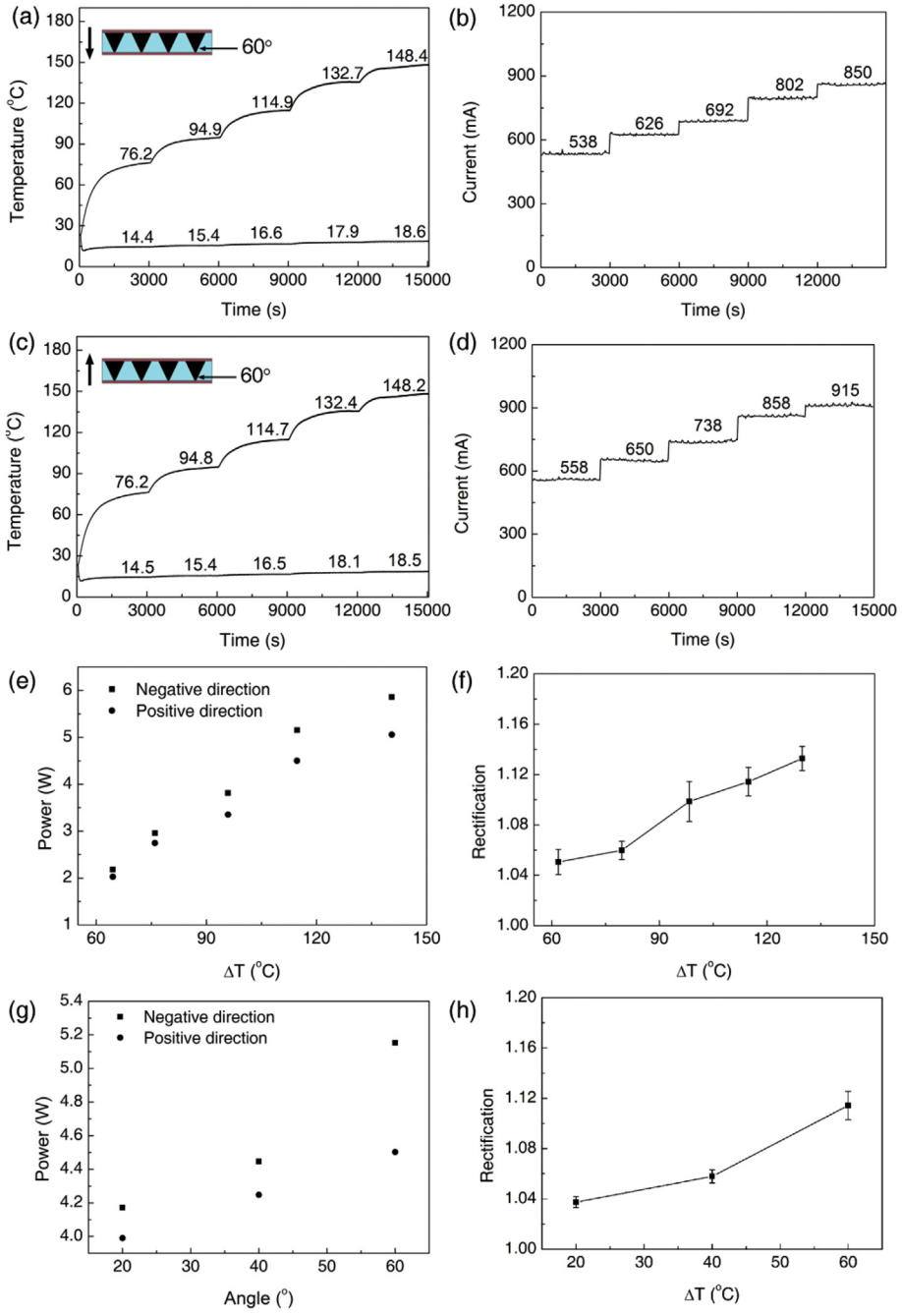

Fig. 4. The monitored top/bottom surface temperature of the PDMS@graphite sample (with the cone angle $\Theta = 60°$) and the electrical currents in heater as a function of time under the (a), (b) positive and (c), (d) negative heating direction. The inset schematics in the top left corner in (a) and (c) depict the positive and negative heat flux in the sample. Measured (e) heater power and (f) thermal rectification coefficient versus the temperature bias ΔT on the sample. In Fig. 4e and f, the first point is $\Delta T_1 = 61.8$ °C ($T_{top} = 76.2$ °C and $T_{bottom} = 14.4$ °C); The second point is $\Delta T_2 = 79.5$ °C ($T_{top} = 94.9$ °C and $T_{bottom} = 15.4$ °C); The third point is $\Delta T_3 = 98.3$ °C ($T_{top} = 114.9$ °C and $T_{bottom} = 16.6$ °C); The fourth point is $\Delta T_4 = 114.8$ °C ($T_{top} = 132.7$ °C and $T_{bottom} = 17.9$ °C); The fifth point is $\Delta T_5 = 129.8$ °C ($T_{top} = 148.4$ °C and $T_{bottom} = 18.6$ °C). Measured (g) heater power and (h) thermal coefficient versus the PDMS@graphite sample with different cone angle ($\Theta = 20°$, 40° and 60°) under the same temperature bias ($\Delta T = 114.8$ °C, the fourth heating step in Fig. 4a and c). (A colour version of this figure can be viewed online.)

was intentionally program controlled to achieve the same temperature bias on the PDMS@graphite sample surfaces as the situation of the positive heating direction. Fig. 4c and d display the experimental sample surface temperature and the electrical current for the heater as a function of time in the negative heating direction, respectively. Obviously, it can be observed that larger electrical current need to be applied to the heater in the negative heating direction to maintain the same temperature bias for the sample. This phenomenon implies that there is thermal rectification effect in our PDMS@graphite system. The input power (P) for the heater can be easily calculated by the following formula:

$$P = r \times I^2 \tag{3}$$

In the experiment, the energy caused by the heater power (P) is not simply equal to the heat transferring across the sample, ascribing to the inevitable heat loss in the measurement process. It

is well known that the thermal transmission, natural convection and radiation are the typical three main heat conduction approaches. In our system, the measurement for the sample was carried out under the vacuum condition, leading to the nearly negligible thermal convection. As for the thermal radiation, the radiation power follows the Stepan-Boltzmann's law written by the below formula [19]:

$$P_{radiation} = \sigma T^4 \times S \quad (4)$$

where the Stepan constant $\sigma = 5.78 \times 10^{-8}$ W m^{-2}. K^{-4}, T is the absolute temperature and S is the surface area of the PDMS@graphite sample, respectively. For the PDMS@graphite sample in our system, the thermal radiation power of the sample is much lower than the total power of the heater and can be treated as negligible. In addition, the thermal insulators are purposely installed between the heater/cooler and the supporting plates in the testing apparatus to effectively prevent the heat leakage. Taking these above negligible heat loss in account, the heat transferring across the PDMS@graphite sample from top to bottom surface can be approximately treated as being equal to the heat caused by the electrical current in the heater. Therefore, the thermal rectification coefficient R can be transformed into the ratio of the negative direction heating power (P_-) to the negative direction heating power (P_+) in the heater as below:

$$R = \frac{|P_-|}{|P_+|} \quad (5)$$

Fig. 4e gives the monitored heating power P_+ and P_- as a function of the temperature bias ($|\Delta T| = |T_{top} - T_{bottom}|$) applied on the top and bottom surface of the PDMS@graphite sample. As displayed in Fig. 4f, the calculated thermal rectification coefficient R monotonically increases from 1.0506 ± 0.009 to 1.1326 ± 0.009 when increasing the applied $|\Delta T|$ on the sample from 61.8 to 129.8 °C in the different heating steps. It should be pointed out that the contact effect can affect the measurement of the thermal rectification [22]. Especially, the effect of a contact is significant when its thickness compares to the order of the size of the rectification system. For our PDMS@graphite composite film thermal rectifier, the thickness of the copper foil tape (0.055 mm) on the top and bottom planar surfaces is much thinner than the thickness of PDMS@graphite composite film in the z direction (4.5 mm). Although the contact effect of copper foil tape will influence the thermal measurements, the total thermal rectification coefficient of PDMS@graphite will be little affected due to the small thickness of copper foil tapes.

3.3. Tuning the thermal rectification coefficient of the PDMS@graphite by changing its asymmetric ratio of the cone-shape interfaces

It has been reported before that the thermal rectification coefficient can be rationally modulated by tuning the asymmetricity ratio of the asymmetric structures in the thermal rectifier [19]. In this work, we also tested the thermal property of PDMS@graphite composite sample with the different cone angle ($\Theta = 20°$ and 40°), in which the height and the spatial distribution of the cone are unchanged but only the cone angle is decreased from 60° to 40° and 20° by decreasing the bottom diameter of the cones. The corresponding Al molds for fabricating PDMS film with cone angle $\Theta = 20°$ and 40° are respectively displayed in Fig. S1 (Supporting Information). Accordingly, Figs. S2 and S3 (Supporting Information) show the dimensions and the spatial distribution of the asymmetric cone-shape graphite with the cone angle $\Theta = 40°$ and 20° in the PDMS@graphite, respectively. Similar testing methods were also taken to investigate the possible thermal rectification effect in PDMS@graphite composite samples with the cone angle 40° and 20°, which are shown in details in Figs. S4 and S5 (Supporting Information). As shown in Figs. S4 and S5, it clearly demonstrates that higher electrical currents are also needed to apply to the heater in the negative heating direction to maintain the same temperature differences $|\Delta T|$ on the sample surface as that of positive heating direction. Being similar to the case of PDMS@graphite composite with cone angle 60°, the calculated thermal rectification coefficient values for the samples with cone angle 20° and 40° also increase with the increment of the $|\Delta T|$ on the samples. Fig. 4g displays the experimental positive and negative direction heat power (P_+ and P_-) for the PDMS@graphite samples with the three different cone angles ($\Theta = 20°$, 40° and 60°) under the same temperature bias ($|\Delta T|$=114.5 °C, the fourth heating step in the testing process). As displayed in Fig. 4h, the corresponding calculated thermal rectification coefficient values increase when enlarging the cone angle in the PDMS@graphite from 20° to 40° and 60°. Combining all these tested results together, it illustrates that the thermal rectification coefficient of the PDMS@graphite composite can be modulated by changing the asymmetry ratio of the cone-shape interface in the sample. If want to further study the thermal rectification coefficient of PDMS@graphite influenced by the cone asymmetricity, the spatial distribution and dimensions of the cone units in PDMS@graphite need to be re-designed and optimized to obtain cone vertex angle larger than 60° or even larger than 90°. Deeper study of the relationship between thermal rectification performance of PDMS@graphite and its cone asymmetricity will be further under investigation in our future work.

3.4. Mechanism of the thermal rectification effect in PDMS@graphite composite film

The first mechanism of the thermal rectification effect in PDMS@graphite is that the averaged thermal conductivity (k) of two components (PDMS and graphite) of the PDMS@graphite sample has the opposite trend of temperature dependence. As pointed out in the previous research about the thermal conductivity of PDMS film using the 3 Ω method [23], the averaged thermal conductivity of PDMS slightly increase from 0.207 to 0.257 W m^{-1}. K^{-1} with increasing the temperature from 22.5 to 100 °C. As for the micrometer sized (particle size smaller than 20 μm) graphite powder in PDMS@graphite, there are many factors to influence its overall thermal conductivity. For example, phonons will collide and scatter at the grain boundaries, lattice defects in graphite powders, which will all finally affect the mean free path of the phonons and thermal conductivity of the graphite powder. Under such low testing temperature (below 200 °C), the phonon (rather than electron and photon) transport mainly contributes to the thermal conduction of the graphite powder in our testing process. Recently, it has been investigated that the averaged thermal conductivity of the micrometer sized graphite powder decreases linearly with increasing the temperature T (relatively low temperature, from room temperature to 200 °C), following below function [24]:

$$K\text{graphite powder}\left(\text{w m}^{-1}\text{°C}^{-1}\right) = 1.27 - 0.003T \quad (6)$$

For the heat flow transferring from graphite to PDMS in the PDMS@graphite sample, segment graphite is relatively hot and segment PDMS is relatively cold. Because k increases with T for segment PDMS but decreases with T for segment graphite, both segments are in a regime of relatively low thermal conductivity. Thus the thermal resistance in this “forward thermal bias” condition is relatively high. When the heat flow direction is reversed, segment graphite becomes relatively cold while segment PDMS is

relatively hot. In this case, both segments have relatively high thermal conductivity, and now the thermal resistance in "reverse thermal bias" is relatively low. Thus, this asymmetric structured PDMS@graphite composite film exhibits thermal rectification effect.

The second mechanism for the thermal rectification effect in PDMS@graphite is the differences of the averaged thermal conductivity (k) of the asymmetric cone-shape graphite embedded in the bulky PDMS@graphite film, which are caused by the different temperature distributions in graphite cones between the forward and backward heating direction when applying the same thermal bias. COMSOL (a finite element program) is employed to simulate the heat flux and temperature distribution in the heating process so as to check the temperature-dependent thermal conductivity in the asymmetric PDMS@graphite system. The corresponding detailed dimensions and above mentioned $K(T)$ relationship for PDMS film and cone-shape graphite in the PDMS@graphite composite are respectively input in the simulation model. In the simulations, we only study the stationary state temperature bias case for the sample. The temperature bias is chosen as $|\Delta T| = 114.5$ °C ($T_{top} = 132.0$ °C, $T_{bottom} = 17.5$ °C) for the PDMS@graphite samples (cone angle $\Theta = 60°, 40°, 20°$), which is very close to the monitored temperature versus time curves in the fourth heating step for the samples. Fig. 5a gives the simulated 3D temperature distribution of the PDMS@graphite sample (cone angle $\Theta = 60°$) in the positive heating direction. Since the totally sixteen cones are evenly distributed in the sample, the typical two-dimensional (2D) temperature distribution on the vertical cross-section along the axis of one row of four cones in the PDMS@graphite can represent temperature distribution differences between PDMS and graphite in the sample (details in Fig. 5b). As displayed in Fig. 5c, it depicts the enlarged 2D temperature distribution configuration on the vertical cross-section along the axis of one typical cone unit in the PDMS@graphite. Similarly, the corresponding simulated temperature distribution results for the PDMS@graphite sample (cone angle $\Theta = 60°$) in the negative heating direction are respectively shown in Fig. 5d–f. Using the same method and temperature bias in the simulations, the simulated temperature distribution results for the cases of PDMS@graphite samples with the cone angle $\Theta = 40°$ and 20° can been found in the details given in Figs. S6 and S7 (Supporting Information). By comparing the simulated temperature distribution results for all these three different kinds of PDMS@graphite samples, it can be obviously observed that larger temperature gradient differences are generated in the graphite powder part in the negative heating direction than that situation in the positive heating direction. Fig. 6 gives the simulated temperature in the axis direction of the cone-shape graphite in the sample (with the different cone angle $\Theta = 20°, 40°, 60°$) as the function of the position, illustrating the higher temperature value at the same position in the positive heating direction than the negative heating direction. Basing on Eq. (6), the averaged thermal conductivity of micrometer sized graphite powder decreases with the temperature. In the negative heating direction, the graphite parts of the PDMS@graphite are under lower "average temperature", leading to higher thermal conductivity and larger heat flux comparing to the situation of positive heating direction. This phenomenon can lead to thermal rectification effect in the PDMS@graphite film. It should be emphasized that the inseparable dependence of thermal conductivity on temperature and space is a necessary condition for thermal rectification in asymmetric geometry bulky single-component material [25,26]. Therefore, the temperature and space dependent thermal conductivity of the asymmetric graphite cones contributes to the asymmetric heat transport of graphite cones in the PDMS@graphite. Finally, it can also be found that sharper differences of temperature distribution in the positive/negative heat flow can be generated in the COMOSL simulations for the PDMS@graphite samples with larger cone angle, which are well consistent with the trends of experimental testing thermal rectification coefficiency of PDMS@graphite with distinct asymmetricity.

There are several advantages for our PDMS@graphite composite thermal rectifier. (1) The PDMS@graphite composite film can realize the thermal rectification effect in the vertical z direction. (2) The PDMS@graphite composite film is flexible and can be transferred on the curved surfaces under particular application occasions. (3) PDMS@graphite composite film can be repeatedly fabricated or scalable by using the Al mold according to the application requirements. It should be mentioned that the flexing effect can influence the thermal rectification performance of PDMS@graphite. If the flexible PDMS@graphite thermal rectifier is bent into curved shape, the geometrical parameters of cone-shape

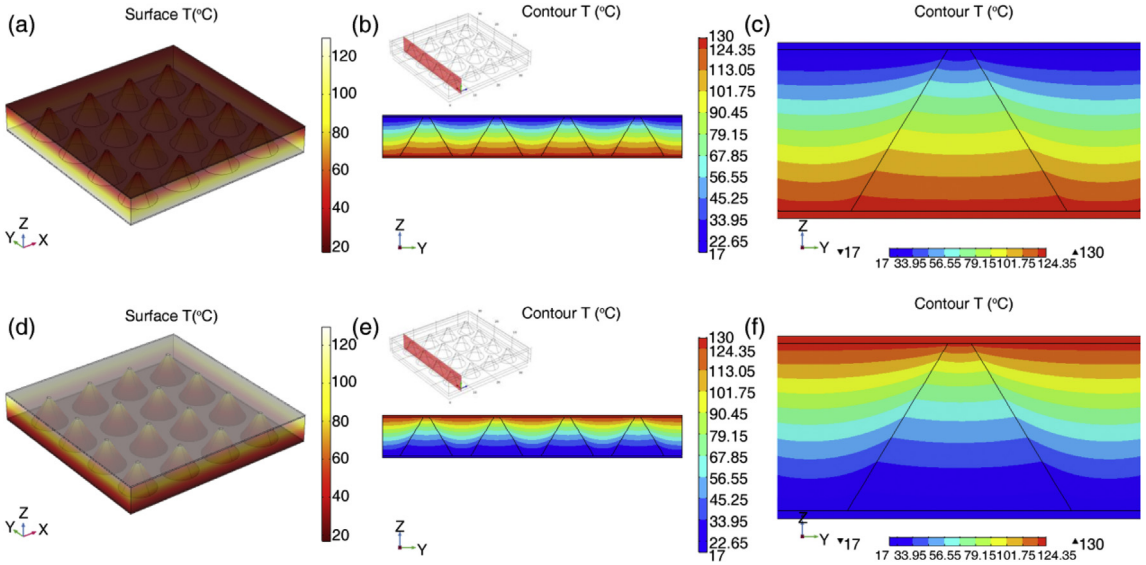

Fig. 5. The COMSOL simulated 3D temperature distribution for the PDMS@graphite (with cone angle $\Theta = 60°$) in (a) positive and (d) negative heating direction. The simulated temperature distribution on one typical cross-section along the axis of a row of cones and one cone unit in PDMS@graphite under the (b, c) positive and (e, f) negative heating direction, respectively. (A colour version of this figure can be viewed online.)

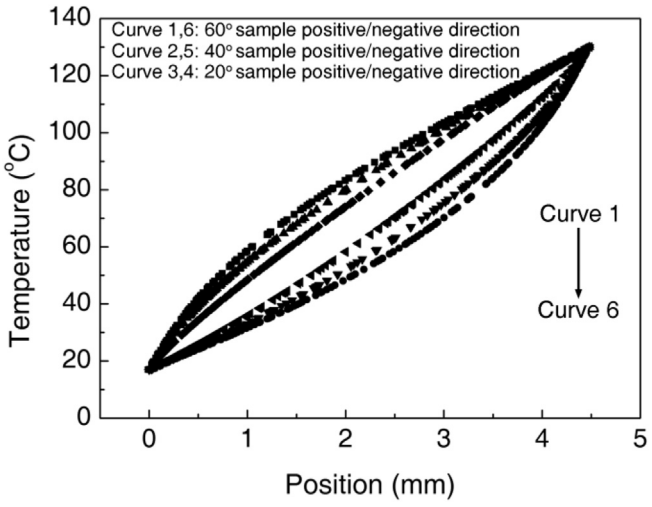

Fig. 6. The COMSOL simulated temperature as a function of position along the axis of the cone in the PDMS@graphite (with cone angle $\Theta = 20^\circ$, 40° and 60°) under the positive and negative heating direction.

graphite and PDMS film will all change comparing to the unbent normal sate, which will cause the corresponding different temperature distributions and distinct averaged thermal conductivity in PDMS and graphite of the PDMS@graphite. These changes will influence the overall thermal rectification coefficiency of PDMS@graphite. Thus, the flexing effect should be taken into consideration and will be further investigated in the future. Basing on the above mentioned mechanisms for the thermal rectification effect of PDMS@graphite composite film, several strategies can be tried to improve the efficiency of this kind of thermal rectifier: (1) preparing this two-segment thermal rectifier by choosing two kinds of materials A and B with shaper thermal conductivity differences in their temperature dependence (comparing to PDMS and graphite); (2) optimizing the asymmetricity, geometrical parameters and the spatial proportion of materials A to B; (3) reducing the interface contact thermal resistance between the materials A and B [16,19]. Our PDMS@graphite composite film provides the reference and prototype to design the thermal rectifier. The further improvement of the thermal rectification efficiency will be under investigation in our future work.

4. Conclusion

In conclusion, a kind of flexible macroscopic thermal rectifier has been achieved in the PDMS@graphite composite film, which is composed of PDMS film with asymmetric cone-shape holes embedded with micrometer sized graphite powder. Experimental results demonstrate that the thermal rectification coefficient of the PDMS@graphite composite can be modulated by tuning of asymmetricity ratio of the cone-shape interfaces in the PDMS@graphite composite. There are two main mechanisms contribute to the thermal rectification in the PDMS@graphite composite system. The one is the opposite temperature dependence of thermal conductivity for PDMS and graphite powder in the PDMS@graphite. The other mechanism is the different temperature-dependent thermal conductivity of asymmetric graphite cones of PDMS@graphite in the positive and negative heating directions under the same temperature bias, which can be demonstrated in the COMOSL theoretical simulations of the temperature distribution in the PDMS@graphite system. The study of the thermal rectification property in PDMS@graphite composite can offer the reference for the design of thermal rectifier with the potential applications in thermal control and management.

Acknowledgments

This work was supported by NTU-A*STAR Silicon Technologies Centre of Excellence under the program Grant (No. 1123510003) and Singapore Ministry of Education Academic Research Fund (Tier 2 No. MOE2013-T2-2-050).

Appendix A. Supplementary data

Supplementary data related to this article can be found at https://doi.org/10.1016/j.carbon.2017.10.046.

References

[1] L. Wang, B. Li, Thermal logic gates: computation with phonons, Phys. Rev. Lett. 99 (2007) 177208.
[2] B.W. Li, L. Wang, G. Casati, Negative differential thermal resistance and thermal transistor, Appl. Rev. Lett. 88 (2006) 143501.
[3] L. Wang, B.W. Li, Thermal memory: a storage of phononic information, Phys. Rev. Lett. 101 (2008) 267203.
[4] Y.Y. Liu, W.X. Zhou, K.Q. Chen, Conjunction of standing wave and resonance in asymmetric nanowires: a mechanism for thermal rectification and remote energy accumulation, Sci. Rep. 5 (2015) 17525.
[5] X. Cartoixa, L. Colombo, R. Rurali, Thermal rectification by design in telescopic Si nanowires, Nano Lett. 15 (2015) 8255–8259.
[6] N. Yang, G. Zhang, B.W. Li, Carbon nanocone: a promising thermal rectifier, Appl. Rev. Lett. 93 (2008) 243111.
[7] G. Wu, B.W. Li, Thermal rectifiers from deformed carbon nanohorns, J. Phys. Condens. Matter 20 (2008) 175211.
[8] N. Yang, G. Zhang, B.W. Li, Thermal rectification in asymmetric graphene ribbons, Appl. Rev. Lett. 95 (2009) 033107.
[9] T. Ouyang, Y.P. Chen, Y.E. Xie, X.L. Wei, K.K. Yang, P. Yang, et al., Ballistic thermal rectification in asymmetric three-terminal graphene nanojunctions, Phys. Rev. B 82 (2010) 245403.
[10] G. Zhang, H.S. Zhang, Thermal conduction and rectification in few-layer graphene Y Junctions, Nanoscale 3 (2011) 4604–4607.
[11] J. Zhu, K. Hippalgaonkar, S. Shen, K.V. Wang, Y. Abate, S. Lee, et al., Temperature-gated thermal rectifier for active heat flow control, Nano Lett. 14 (2014) 4867–4872.
[12] C.W. Chang, D. Okawa, A. Majumdar, A. Zettl, Solid-state thermal rectifier, Science 314 (2006) 1121–1124.
[13] E. Pallecchi, Z. Chen, G.E. Fernandes, Y. Wan, J.H. Kim, J. Xu, A thermal diode and novel implementation in a phase-change material, Mater. Horiz. 2 (2015) 125–129.
[14] R.J. Chen, Y.L. Cui, H. Tian, R.M. Yao, Z.P. Liu, Y. Shu, et al., Controllable thermal rectification realized in binary phase change composites, Sci. Rep. 5 (2015) 8884.
[15] W. Kobayashi, Y. Teraoka, I. Terasaki, An oxide thermal rectifier, Appl. Rev. Lett. 95 (2009) 171905.
[16] D. Sawaki, W. Kobayashi, Y. Moritomo, I. Terasaki, Thermal rectification in bulk materials with asymmetric shape, Appl. Rev. Lett. 98 (2011) 081915.
[17] Y. Li, X.Y. Shen, Z.H. Wu, J.Y. Huang, Y.X. Chen, Y.S. Ni, et al., Temperature-dependent transformation thermotics: from switchable thermal cloaks to macroscopic thermal diodes, Phys. Rev. Lett. 115 (2015) 195503.
[18] X.M. Gu, S.D. Zhang, M.Y. Shang, T.T. Zhao, N. Li, H.F. Li, et al., Asymmetric geometry composites arranged between parallel aligned and interconnected graphene structures for highly efficient thermal rectification, RSC Adv. 7 (2017) 10683–10687.
[19] H. Tian, D. Xie, Y. Yang, T.L. Ren, G. Zhang, Y.F. Wang, et al., A novel solid-state thermal rectifier based on reduced graphene oxide, Sci. Rep. 2 (2012) 523.
[20] Y.J. Jung, S. Kar, S. Talapatra, C. Soldano, G. Viswanathan, X.S. Li, et al., Aligned carbon nanotube-polymer hybrid architectures for diverse flexible electronic applications, Nano Lett. 6 (2006) 413–418.
[21] K.J. Regehr, M. Domenech, J.T. Koepsel, K.C. Carver, S.J. Ellison-Zelski, W.L. Murphy, et al., Biological implications of polydimethylsiloxane-based microfluidic cell culture, Lab. Chip 9 (2009) 2132–2139.
[22] T. Majdi, S. Pal, I.K. Puri, Recipe for optimizing a solid-state thermal rectifier, Int. J. Therm. Sci. 117 (2017) 260–265.
[23] P.Y.C.N. Al-Khudary, Y. Orlic, P. Coquet, P. Pernod, T. Lasri, Measurement of the thermal conductivity of polydimethylsiloxane polymer using the three omega method, Key Eng. Mater 613 (2014) 259–266.
[24] E.M. Moon, C. Yang, V.V. Yakovlev, Microwave-induced temperature fields in cylindrical samples of graphite powder-experimental and modeling studies, Int. J. Heat. Mass Tran 87 (2015) 359–368.
[25] Y. Wang, A. Vallabhaneni, J.N. Hu, B. Qiu, Y.P. Chen, X.L. Ruan, Phonon lateral confinement enables thermal rectification in asymmetric single-material nanostructures, Nano Lett. 14 (2014) 592–596.
[26] N.A. Roberts, D.G. Walker, A review of thermal rectification observations and models in solid materials, Int. J. Therm. Sci. 50 (2011) 648–662.